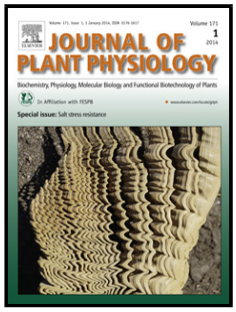

Title: Deregulation of Apoplastic POLYAMINE OXIDASE affects development and salt response of tobacco plants

Authors: Katalin Gémes, nullfigeneia Mellidou, Katerina Karamanoli, Despoina Beris, Ky Young Park, Theodora Matsi, Kosmas Haralampidis, Helen-Isis Constantinidou, Kalliopi A. Roubelakis-Angelakis

PII: S0176-1617(17)30011-1
DOI: http://dx.doi.org/doi:10.1016/j.jplph.2016.12.012
Reference: JPLPH 52503

To appear in:

Received date: 3-9-2016
Revised date: 15-12-2016
Accepted date: 19-12-2016

Please cite this article as: Gémes Katalin, Mellidou x399;figeneia, Karamanoli Katerina, Beris Despoina, Park Ky Young, Matsi Theodora, Haralampidis Kosmas, Constantinidou Helen-Isis, Roubelakis-Angelakis Kalliopi A.Deregulation of Apoplastic POLYAMINE OXIDASE affects development and salt response of tobacco plants.*Journal of Plant Physiology* http://dx.doi.org/10.1016/j.jplph.2016.12.012

Deregulation of Apoplastic POLYAMINE OXIDASE affects development and salt response of tobacco plants

Katalin Gémes[1,2], Ifigeneia Mellidou[3], Katerina Karamanoli[3], Despoina Beris[4], Ky Young Park[5], Theodora Matsi[3], Kosmas Haralampidis[4], Helen-Isis Constantinidou[3]*, Kalliopi A. Roubelakis-Angelakis[1]*

[1]Department of Biology, University of Crete, Voutes University campus, 70013 Heraklion, Greece

[2]Biological Research Centre, Hungarian Academy of Sciences, H-6726 Szeged, Temesvari krt. 62, Hungary

[3]School of Agriculture, Aristotle University, 54124 Thessaloniki, Greece

[4]Department of Biology, National and Kapodistrian University of Athens

[5]Department of Biology, Sunchon National University, 57922, Chonnam, South Korea

*__Corresponding authors__: poproube@biology.uoc.gr; constad@agro.auth.gr

Keywords: Polyamine Oxidase; Sense/antisense PAO transgenics; ion content under salinity; net photosynthesis; oxidative stress; salt tolerance.

Abbreviations: PAs, polyamines; PAO, Polyamine oxidase; WT, Wild type tobacco; *S-ZmPAO/AS-ZmPAO*, Sense/Antisense-*ZmPAO* transgenic plants; A_{net}, Net photosynthetic rate; CCI, Chlorophyll content index; DAT, Days after treatment; FW, Fresh weight; DW, Dry weight; FRAP, Ferric reducing antioxidant power; LA, Leaf area; QY, Quantum yield of PSII; REL, Root electrolyte leakage; ROS, Reactive oxygen species.

Acknowledgments

This research was funded by the EU and the Greek national funds, research funding program THALES (MIS 377281 to K.A.R.-A.), and by Korea Research Institute of Bioscience and Biotechnology (to K.Y.P.). It was implemented in the frame of COST Action FA1106. The authors thank Dr Panagiotis N. Moschou and Dr Imene Toumi for their assistance in the lab of K.A.R.-A. Correspondence should be sent to K.A.R.-A. (poproube@biology.uoc.gr) or to H.-I. C. (constad@agro.auth.gr).

Summary

Polyamine (PA) homeostasis is associated with plant development, growth and responses to biotic/abiotic stresses. Apoplastic PA oxidase (PAO) catalyzes the oxidation of PAs contributing to cellular homeostasis of reactive oxygen species (ROS) and PAs. In tobacco, PAs decrease with plant age, while apoplastic PAO activity increases. Our previous results with young transgenic tobacco plants with enhanced/reduced apoplastic PAO activity (S-*ZmPAO*/AS-*ZmPAO*, respectively) established the importance of apoplastic PAO in controlling tolerance to short-term salt stress. However, it remains unclear if the apoplastic PAO pathway is important for salt tolerance at later stages of plant development. In this work, we examined whether apoplastic PAO controls also plant development and tolerance of adult plants during long-term salt stress. The AS-*ZmPAO* plants contained higher Ca^{2+} during salt stress, showing also reduced chlorophyll content index (CCI), leaf area and biomass but taller phenotype compared to the wild-type plants during salt. On the contrary, the S-*ZmPAO* had more leaves with slightly greater size compared to the AS-*ZmPAO* and higher antioxidant genes/enzyme activities. Accumulation of proline in the roots was evident at prolonged stress and correlated negatively with *PAO* deregulation as did the transcripts of genes mediating ethylene biosynthesis. In contrast to the strong effect of apoplastic PAO to salt tolerance in young plants described previously, the effect it exerts at later stages of development is rather moderate. However, the different phenotypes observed in plants deregulating *PAO* reinforce the view that apoplastic PAO exerts multifaceted roles on plant growth and stress responses. Our data suggest that deregulation of the apoplastic PAO can be further examined as a potential approach to breed plants with enhanced/reduced tolerance to abiotic stress with minimal associated trade-offs.

Introduction

Salinity is a major abiotic threat to global agriculture due to increasing use of poor quality water for irrigation and soil salinization. The highly reactive aliphatic polycations named polyamines (PAs), the di-amine putrescine (Put), the tri-amine spermidine (Spd) and the tetra-amine spermine (Spm) affect developmental and metabolic processes, as well as a vast range of stress responses. PAs homeostasis is maintained by the fine orchestration of biosynthesis, conjugation, compartmentalization, transport and oxidation/back-conversion. The apoplastic flavoprotein PA oxidase (PAO) oxidizes Spd yielding Δ^1- pyrroline and Spm yielding 1,5-diazabicyclononane, along with 1,3-diaminopropane (1,3-Dap) and H_2O_2, affecting PA and H_2O_2 homeostasis, and the ratio of biosynthesis/ catabolism (Mattoo et al., 2006; Moschou et al., 2008c; Moschou et al., 2009).

Previously, we used young tobacco transgenic seedlings with increased (S-*ZmPAO;* overexpressing *ZmPAO*) and reduced apoplastic PAO activity (AS-*ZmPAO*; overexpressing the antisense cDNA from *ZmPAO* that blocks translation of tobacco PAO; Moschou et al., 2008a,b) to study the effect of apoplastic PAO to salinity. Salinity or pathogens induce Spd exodus and oxidation in the apoplast which significantly contributes to regulation of H_2O_2 'signatures' defining the outcome of stress responses (Moschou et al., 2009; Moschou and Roubelakis-Angelakis, 2014). NADPH-oxidase and the apoplastic PAO constitute a feedforward ROS amplification loop, which impinges on oxidative state and culminates in the execution of programmed cell death (PCD). The data suggest that this loop is a central hub in the plethora of responses controlling salt stress tolerance, with potential functions extending beyond stress tolerance (Gémes et al., 2016). S-*ZmPAO* transgenic tobacco plants show increased inter-/intracellular levels of the reactive oxygen species (ROS) H_2O_2 and $O_2^{\cdot -}$ and expression of antioxidant genes, which are nevertheless insufficient to scavenge these ROS efficiently (Moschou et al., 2008a, 2008b). The *AS-ZmPAO* tobacco young seedlings show tolerance to short-term salt stress, either due to increased PA content or decreased ROS levels from the impaired PA oxidation in the apoplast (Moschou et al., 2008a, 2008b).

Given that the severity/mode(s) of response(s) to stress are cell/tissue/organ but also ontogenetic stage-specific processes, we assessed tolerance and examined growth characteristics of adult S-*ZmPAO* and AS-*ZmPAO* plants under control conditions or during long-term salt treatments. We also determined photosynthetic parameters, the intracellular monovalent and divalent cation contents, under prolonged/varying salt stress,

and also the efficiency of the antioxidant enzymes and machinery. Our results highlight the developmental stage-specific role of apoplastic PAO in the regulation of development and plant responses to salt stress.

Materials and Methods

Plant material, growth conditions and salt treatments

Partial cDNA cloning of the *PAO* gene (Yoda et al., 2006), vector construction, plant transformation and molecular analysis of the transgenics were described by Moschou et al. (2008a, 2008b). Plants of WT (*Nicotiana tabaccum* cv Xanthi) and the transgenic lines S2.2 and A2, over-/downexpressing the *ZmPAO* gene, respectively (Moschou et al., 2008a, 2008b) were used. These lines from now-on will be referred as S-*ZmPAO* and AS-*ZmPAO*. The plants were grown as described earlier (Mellidou et al., 2016). In brief, seeds from the three genotypes were cold stratified (4 °C, 7 days), and immersed in a 1 % potassium nitrate solution for 12 h. Then, the seeds were sown in 10-cm diameter pots filled with peat (Terraplant, Compo) and perlite (2:1; v/v) mixture, and placed under plastic cover for 3 d to preserve high relative humidity. At the four-true-leaf stage, 120 seedlings per genotype were transplanted in 0.25 L pots, filled with the aforementioned mixture and placed in a completely randomised design (split-split-plot arrangement). At the 4-5 pair true leaf stage (70 day-old plants), five salt treatments (0, 50, 100, 200, 300 mM NaCl) were applied, each on 24 plants per genotype. All plants were subjected to salt treatment through irrigation either with 100 mL aqueous solution of the respective NaCl dose or with 100 mL water (controls) at 0, 4, 7, 11, 14 and 18 days after the first treatment (DAT). At four sampling times (0, 7, 14, 21 DAT) six plants/genotype-treatment (each considered as a single replication) were harvested. Growth, developmental and physiological characteristics were evaluated on three plants and phytochemical parameters were determined on the other three.

In addition, seeds were surface sterilised with bleach for 10 min, washed four times with sterile water and plated on filter paper in plates with 1/2Murashige and Skoog medium [Duchefa Biochemie, Haarlem, Netherlands; supplemented with 0.05 % MES/KOH, pH 5.7 (2-(*N*-morpholino) ethanesulfonic acid) (Sigma-Aldrich, St. Louis MO, USA), Gamborg B5 vitamins and micronutrient mixture (Duchefa), 2 % (w/v) sucrose]. Seedlings were grown in a growth chamber for 13 days. Seedlings were transplanted in plates with the same medium containing 0 or 100 mM NaCl for 2 more

days before being used. All plants were grown under long day conditions (16/8 h photoperiod) at 22/18 °C, and 110 $\mu Em^{-2}s^{-1}$ PAR supplied by cool-white fluorescent tungsten tubes (Osram, Berlin, Germany).

RNA extraction and semi-quantitative RT-PCR and q-RT-PCR

Total RNA isolation and RT-PCR were performed as described earlier (Mellidou et al., 2016). Conditions of PCR amplification were as follows: 2 min at 94 °C, 1 min at 92 °C, 1 min at the appropriate annealing temperature, 35 s at 72 °C, and a final extension step of 5 min at 72 °C. All amplicons were separated by 1.4 % (w/v) agarose gel electrophoresis, stained with EtBr and visualised under UV light. The total density of individual bands was measured with GelEval software package (v1.37, Frog Dance Software). In addition, to q-RT-PCR, isolation of total RNA was performed as previously described (Wi and Park, 2002). One μg of total RNA from leaves was reverse-transcribed for 30 min at 42 °C in a 20 μL reaction volume using a High Fidelity PrimeScript^{TM} RT-PCR kit (Takara, Japan) according to the manufacturer's instructions. The q-RT-PCR reactions were carried in Chromo 4^{TM} Continuous Fluorescence Detector (Bio-Rad, USA). Ct values were analyzed using MJ Opticon Monitor Software version 3.1 (Bio-Rad, USA) and then exported to Microsoft Excel for further analysis. The reference gene *β-ACTIN* was used. The primers used appear in Suppl. Table 1.

Protein extraction and In-gel enzyme assays

Proteins were extracted and treated as described in Papadakis and Roubelakis-Angelakis (2005). For native electrophoresis and enzyme activity stainings, proteins were electrophoretically resolved using native PAGE and then stained. For SOD activity staining the procedure was carried out according to Andronis et al. (2014). SOD enzyme activity was determined by incubating the gel in 50 mM potassium phosphate buffer (pH 7.4) containing 2 mg/mL NBT for 30 min in dark, and then in another 50 mM potassium phosphate buffer (pH 7.4) containing 0.1 mg/mL riboflavin and 0.25 % TEMED for 20 min in dark. The gel was placed into distilled water in light until bands were detected.

Ion content

Ion content (K^+, Na^+, Ca^{2+}, and Mg^{2+}) was determined in shoots of AS-*ZmPAO*, S-*ZmPAO* transgenic and WT plants grown in the presence of 0, 50, 100, 200, and 300 mM

NaCl at 0, 7, 14 and 21 DAT as already reported (Mellidou et al., 2016). The monovalent ions (K^+ and Na^+) were determined with a flame photometer (Jenway PFP 7, Gransmore Green, Felsted England), and the divalent ones (Ca^{2+} and Mg^{2+}) with an atomic absorption spectrophotometer (Shimadzu AA 6300, Japan).

Photosynthetic Parameters: photosynthetic yield, chlorophyll content index and net photosynthesis

In an attempt to assess to what extent deregulation of *PAO* affects photosynthetic efficiency, photosynthetic yield [effective quantum yield of photochemical energy conversion in photosystem II or simply quantum yield (QY)], chlorophyll content index (CCI= % transmittance at 931nm/ % transmittance at 653nm) and net photosynthetic rate (A_{net}, μmol $m^{-2}s^{-1}$) were determined in AS-*ZmPAO*, S-*ZmPAO* transgenics and WT plants, on the fifth fully expanded leaf (counting from the apex) of 70 day-old plants (time 0), subsequently of 77, and 84 day-old plants (7 and 14DAT) grown in the presence of 0, 50, 100, 200, and 300 mM NaCl, as described before (Mellidou et al., 2016). For these determinations we used a portable photosynthesis system (LI-6200, LI-COR Inc. Lincon NE, USA), a direct portable fluorometer (Photosynthesis yield analyzer MINI–PAM, Walz, Effeltrich, Germany), and an Opti-Sciences CCM-200 chlorophyll content meter (OptiSciences Inc., Tyngsboro MA). Also, QY was computed in terms of the efficiency of the energy harvesting by open PSII reaction centres in the light, as previously described (Kadoglidou et al., 2014). For both QY and CCI, ten measurements were taken per genotype and treatment at each sampling day. To avoid photoinhibition, all physiological measurements were performed in a 2 h time span, approximately 3 h after sunrise.

Plant Phenology: plant height, leaf number, leaf area, fresh and dry weight

Since photosynthetic rate and efficiency directly affect plant growth and development, several phenotypic characteristics were assessed in AS-*ZmPAO*, S-*ZmPAO* transgenic and WT plants, using 70 day-old plants (time 0), subsequently of 77, 84, and 91 day-old plants (0, 7, 14, 21 DAT) at 0, 50, 100, 200, and 300 mM NaCl, as already described (Mellidou et al., 2016). The plant height from the soil surface to the base of the petiole of the youngest fully expanded leaf was recorded, the leaves were counted and removed from the stems for further use. The leaf area (LA) was evaluated from digital images acquired using a flatbed scanner. The images were analyzed applying the software

ImageJ (Schneider et al., 2012). The samples (leaves and stems) were oven-dried at 70 °C till stable weight and their dry weight was recorded.

Total Soluble Phenolics and Antioxidant Activity

In addition to enzymatic antioxidant machinery, cells employ non-enzymatic antioxidants for protection from excessive ROS, such as phenolics. Quantification of total soluble phenol content and antioxidant activity was performed over a 14 DAT period in WT and transgenic plants treated with 100 mM NaCl as described in Mellidou et al. (2016). In addition, total phenolics were determined qualitatively in leaf tissues from plants treated with 100 mM NaCl for 24 h. In addition, in order to dissect whether changes in endogenous phenolics are actually induced by osmotic or ionic stress, mannitol treatment was also used at 100 mM, and total phenolics in the leaves were determined at 0, 7, 14 DAT and compared with the effect of 100 mM NaCl. Phenolics were extracted according to Tsiri et al. (2009), qualitatively analyzed by Thin Layer Chromatography (TLC), visualized under UV light after staining and quantified using the aluminium chloride colorimetric method as described in Mellidou et al. (2016). The total antioxidant activity of the leaves was determined as the ferric reducing antioxidant potential (FRAP) (Benzie et al., 1999) in MeOH leaf extracts prepared similarly to the determination of total phenolics (Mellidou et al., 2016). Absorbance of the mixture was read at 593 nm with a UV-Vis spectrophotometer (Shimadzu UV-1601). Results were expressed on a fresh weight basis as ascorbic acid equivalents (AAE).

Proline and Root Electrolyte Leakage in Roots

Salinity is known to cause osmotic/ionic stress to plant cells and the amino acid proline is a common osmoprotectant. Proline content in roots of the 3 genotypes was determined as described by Bates et al. (1973). Briefly, 500 mg of root material was homogenized in 5 mL of 3 % aqueous sulfosalicylic acid. After centrifugation for 10 min at 12,000 g, 2 mL of the supernatant was left to react with 2 mL acid ninhydrin and 2 mL acetic acid in a test tube for 1 h at 100 °C. The reaction mixture was extracted twice with 4 mL toluene, and the absorbance of the extract read at 520 nm with a UV-Vis-spectrophotometer (Shimadzu UV-1601) using toluene as blank. Proline content was expressed on a fresh weight basis.

Electrolyte leakage (REL) from roots was determined using the relative conductivity method as modified by McKay (1998). Root samples (100 mg) were

thoroughly washed with cold tap water to remove soil and then added to 25 mL test tubes containing 15 mL of distilled water of a known conductivity. The tubes were well shaken in a vortex and left at room temperature in the dark for 24 h. The next day, the tubes were shaken again and the conductivity of the bathing solution was measured. Then, the samples were boiled at 110 °C for 20 min, let to cool at room temperature, and total conductivity of the bathing solution was again measured. REL was expressed as a percentage of the conductivity after boiling and after subtracting the conductivity of distilled water before boiling. Three replicates were used per genotype and treatment at each sampling time.

Statistical analysis

The experiments were established in a completely randomized pattern in a split-split-plot arrangement, with the genotype, the NaCl dose and the sampling time as independent factors. Each combined factor had three replicates in all parameters except for the CCI and QY that had 10 replicates. Statistical analysis was carried out with SIGMAPLOT12.0 statistical software. After ANOVA, Duncan's multiple comparisons were performed. Student's test was done using JMP (SAS, version 11 pro). Multiple average comparisons, graphs and data processing were performed in EXCEL and SIGMAPLOT12.0.

RESULTS

Deregulation of *PAO* gene affects plant phenotype under normal and salt stress conditions

Here, we assessed the effect of deregulation of apoplastic PAO on the phenotype of adult tobacco plants under control conditions or during salinity. In particular, we performed a comparative study of 70 day-old WT, S-*ZmPAO* and AS-*ZmPAO* plants at 0 (control), 7, 14 and 21 days post-treatment (DAT) with 0 (control), 50, 100, 200, and 300 mM NaCl. The AS-*ZmPAO* plants tended to show taller phenotype whereas the S-*ZmPAO* plants showed no significant change under control conditions (0 DAT and 0 mM NaCl) compared to WT plants (Fig. 1A). However, this phenotype of AS-ZmPAO was not retained at later stages (14, 21 DAT). Plant height decreased with increasing salt in a dose-dependent manner in all genotypes, but still the AS-*ZmPAO* plants continued to show taller phenotype, especially at 300 mM salt, when the height reduction was 44.0 %

in WT, 45.6 % in S-*ZmPAO*, and only 19.7 % in the AS-*ZmPAO* compared to the controls at 21 DAT (Fig. 1A).

The S-*ZmPAO* plants showed increased number of leaves under salinity conditions (50 and 100 mM) (Fig. 1B). However, at 200 and 300 mM the number of leaves was almost the same in all genotypes. At 300 mM/21 DAT the reduction of leaf number compared to the controls was 32.7 % in WT, whereas in S-*ZmPAO* and AS-*ZmPAO* it was only 1.1 % and 5.0 %, respectively. Salinity reduced leaf area in all genotypes, mostly in the AS-*ZmPAO* (51.4 % at 21 DAT/300 mM NaCl) (Fig. 1C). Nearly at all treatments and time points the leaf area of AS-*ZmPAO* plants was smaller than that of WT/S-*ZmPAO*, and this effect was not dependent on stress. Our results suggest that apoplastic PAO is required to sustain leaf expansion during normal conditions, which results to an opposite effect in the plant height.

The fresh weight (FW) of the aerial parts of AS-*ZmPAO* at 0 mM NaCl was significantly lower than that of WT and S-*ZmPAO* (Fig. 2A). Salt treatments resulted to reduced FW with the same trend in all genotypes/salt doses and time points (Fig. 2A). Again, AS-*ZmPAO* plants showed the lowest biomass while the S-*ZmPAO* plants were also significantly affected. When biomass was expressed as dry weight (DW), similar but less marked trends were found. Salinity resulted to reduced DW in all genotypes in a dose-responsive manner (Fig. 2B). Apparently, the reduced cell expansion and leaf area in AS-*ZmPAO* is reflected in the reduced weight.

Changes in growth parameters do not correlate with photosynthetic efficiency

Next, we assessed the correlation between phenotypic and photosynthetic characteristics. Under control conditions (0 mM NaCl/0 DAT) all genotypes showed similar values of QY and CCI, whereas at 0 mM NaCl/7 DAT both transgenics exhibited significantly greater A_{net} which nevertheless was nullified at 14 DAT (Fig. 3A,B,C). In fact, under control conditions (0 mM NaCl/0 DAT), QY and CCI were rather equal in all genotypes as did QY under salinity. Under 50 and 100 mM NaCl at 14 DAT, CCI was greater in the WT than in the transgenics, but not under 200 and 300 mM NaCl/14 DAT (Fig. 3A,B). Interestingly, the AS-*ZmPAO* genotype in all salt treatments at 7 DAT, showed a marked decrease in the A_{net}, suggesting an osmotic/ionic shock, which was overcome 14 DAT (Fig. 3C). Taken all together, the results do not reveal a clear picture on the effect that deregulation of PAO exerts on these photosynthetic parameters.

Deregulation of apoplastic PAO seems to affect foliar ion content

PAs play a major role in controlling ion homeostasis (Shabala and Pottosin, 2014; Pottosin, 2015). In all genotypes Ca^{2+} and Mg^{2+} levels showed a positive correlation with leaf age, while K^+ levels decreased with age and Na^+ levels were not significantly affected (Fig. 4A,B,C,D/0 mM/0-21 DAT). AS-*ZmPAO* plants showed increased levels of K^+, Ca^{2+} and Mg^{2+} at 0 mM NaCl, at most time points examined (with the exception of Mg^{2+} and Ca^{2+} at 0 DAT/0 mM NaCl) compared to WT. In particular, the levels of K^+ were greater in the control AS-*ZmPAO* plants at most time-points (Fig. 4B). Treatment with 50 to 300 mM NaCl resulted to significant increase of Na^+, which accumulated in the leaf tissue in a time/dose-dependent manner in all genotypes. At the highest salt dose and some time points, the AS-*ZmPAO* leaves accumulated less Na^+ compared to WT (Fig. 4A). Under salt, the content of foliar K^+ in the AS-*ZmPAO* did not show a consistent profile of change, compared to WT and S-*ZmPAO* (Fig. 4B). The content of Mg^{2+} decreased in AS-*ZmPAO* almost at WT-levels after salt stress, while Ca^{2+} was significantly higher under the same conditions (Fig. 4C,D). Taken together, our results suggest that apoplastic PAO affects steady-state ion contents in a rather complex manner, under both, control and salt stress conditions.

Apoplastic PAO regulates ROS homeostasis mainly through Ascorbate peroxidase

The mRNA levels of the H_2O_2-producing O_2.- dismutases *CuZnSOD*, the FeSOD/MnSOD isoenzymes and their respective in-gel activity were determined. The S-*ZmPAO* genotype showed the highest levels of *CuZnSOD* mRNA (Fig. 5A) and activities of FeSOD/MnSOD isoenzymes (Fig. 5B-D). We also assesed the mRNA abundance of the main H_2O_2-scavenging enzymes, ascorbate peroxidase (APX; high affinity to H_2O_2, active at low concentrations of H_2O_2) and catalase (CAT; low affinity to H_2O_2, active at high concentrations of H_2O_2; Fig. 5E,F). More specifically, we estimated mRNA levels of the most reactive to PAO-deregulation APX isoform in S-*ZmPAO*, the cytoplasmic one (*APXc*; Davletova et al., 2005; Moschou et al., 2008a). At 0 h, a slight induction of the *APXc* mRNA levels was observed in AS-*ZmPAO* and S-*ZmPAO* (Fig. 5E; 0 h). The mRNA levels of *APXc* peaked in all three genotypes 6h post-NaCl treatment and declined thereafter (Fig. 5E; 6 and 24 h). The S-*ZmPAO* plants showed the highest mRNA levels of *APXc*, at 6 h post- NaCl treatment (Fig. 5E; 6 h) in accordance with the higher ROS levels in this genotype, while the AS-*ZmPAO* showed the lowest mRNA levels (Moschou et al., 2008b; Gémes et al., 2016). Under control conditions *CAT1* mRNA levels did not differ

among the three genotypes, whereas a profound increase of *CAT1* mRNA levels was observed 1 h post-treatment with NaCl in all three genotypes (Fig. 5F; 1 h), and increased further at 24 h post-treatment in WT and mostly in S-*ZmPAO*. These data confirm the tight association of PAO levels with antioxidant machinery.

Next, we assessed total phenolics, potent non-enzymatic antioxidants. Deregulation of *PAO* did not alter the total phenolic content at 0 DAT. Interestingly, endogenous phenolics increased in a developmentally-dependent manner. It increased 3 to 5-fold with age mostly in S-*ZmPAO* (20% higher than WT at 7 DAT). Treatment with salt (100 mM) did not affect phenolic titers in the WT, whereas it caused a significant reduction in S-*ZmPAO* and to a lesser extent in the AS-*ZmPAO* (Fig.6A/100 mM NaCl/ 7 DAT). The effect of mannitol on total phenolics was very similar to that of NaCl (Fig. 6B). The TLC qualitative profile was affected neither by the deregulation of PAO nor by the treatment with 100 mM NaCl/24h (Fig. 6C). When the total antioxidant activity (Ascorbic Acid Equivalents, AAE) was assessed, the WT showed lower AAE compared to both transgenics, which exhibited comparable values (Fig. 6D). Our results suggest that phenolics are not regulated by PAOs, while the increase in S-*ZmPAO* at control conditions may represent a rather compensatory mechanism in an attempt to restore ROS homeostasis.

Deregulation of *PAO* affects the mRNA levels regulating ethylene biosynthesis

PAs and ethylene share a common precursor, S-adenosyl-L-methionine. We postulated that the deregulation of PAs homeostasis could affect the ethylene biosynthetic machinery and the induction of ethylene could be related to PAO (Hou et al., 2013). Thus, it was of interest to assess whether or not deregulation of *PAO* would affect the ethylene biosynthetic genes under NaCl stress. Overall, the levels of mRNAs of the genes coding for ACC (1-aminocyclopropane-1-carboxylate) synthase (*ACCSyn*) and ACC oxidase (*ACCOx*) showed higher mRNA levels in the AS-*ZmPAOi*, in all time points examined compared to S-*ZmPAO*, while WT showed the lowest levels (Fig. 7). More specifically, under control conditions, the mRNA levels were nearly 4- and 8-fold higher in the AS-*ZmPAO* genotype compared to the WT (Fig. 7), whereas in the S-*ZmPAO* the respective increases were 2- and 3-fold for *ACC oxidase/ACC synthase*, respectively (Fig. 7). Upon NaCl treatment, the abundance of both mRNAs showed minor decreases throughout the 72 h period in the AS-*ZmPAO* with similar trend in the S-*ZmPAO* genotype. On the contrary, in WT both mRNAs continued increasing. The results support

that deregulation of *PAO* gene affects the expression of the main biosynthetic genes of ethylene possibly *via* the altered homeostasis of PAs in the transgenic plants.

Proline accumulates in the roots only 7 DAT onward at high salt and does not correlate with REL

In an effort to examine whether accumulation of the osmolyte proline and root electrolyte leakage (REL) differ among the WT and PAO transgenics, we determined the content of proline and assessed the root membrane integrity by REL. No particular difference between genotypes was observed up to 100 mM NaCl (data not shown). Interestingly, proline started accumulating at 7 DAT in a dose-dependent manner. At 14 DAT proline was rather unaffected under 200 mM NaCl whereas it reached a 4-fold increase in all genotypes at 300 mM NaCl. Twenty-one days post-treatment with 200 mM NaCl, all genotypes exhibited increased proline. WT and S-*ZmPAO* plants tended to accumulate higher proline compared to AS-*ZmPAO*, while WT accumulated higher proline compared to the transgenic genotypes at 300 mM NaCl (Fig. 8A) At control conditions there was no significant difference in REL among the genotypes (Fig. 8B/0 DAT) and no correlation was found between proline content and the REL. For instance, the higher proline in the WT at 300 mM/21 DAT, was not accompanied by lower electrolyte leakage (Fig. 8B).

Discussion

Low PA mutants exhibit increased sensitivity to salt stress linking PA homeostasis with salt tolerance. For example, the PA biosynthesis *Arabidopsis* loss-of-function *adc2* mutant which contains about 25 % lower Put than WT plants, shows higher sensitivity to salt stress than the WT (Urano et al., 2005). Likewise, the *Arabidopsis* loss-of-function mutant *acl5spms* that is unable to produce Spm is hypersensitive to salt stress (Yamaguchi et al., 2006). Tobacco plants with reduced activity of SAMDC, a biosynthetic enzyme of Spd and Spm show increased biomass, height and leaf number, but are hypersensitive to salt stress. These plants are unable to control H_2O_2 levels and concentrations of monovalent and divalent cations (Mellidou et al., 2016).

Apoplastic PAO drives cell elongation during salt stress in maize (Rodríguez et al., 2009; Shoresh et al., 2011; Swanson and Gilroy, 2010). In this study, we observe a decrease in leaf size of AS-*ZmPAO* tobacco plants under control and salt stress conditions. On the contrary, the S-*ZmPAO* plants show increased leaf area, at least

transiently, although this effect is not sustained under salt stress (Fig. 1A,B,C). This is consistent with the increased sensitivity of these plants that has been described before at earlier stages of plant development (Moschou et al., 2008a, 2008b). Young AS-*ZmPAO* seedlings, which contain higher PAs and lower ROS under short-term salinity stress, show increased biomass (Moschou et al., 2008b). However, the adult plants under prolonged stress periods, show lower biomass, but significantly taller phenotype (Fig. 1A, 2A; Moschou et al., 2008a, 2008b).

Increased vigour has been associated with enhanced photosynthesis (Fujimoto et al., 2012). Photosynthetic response to salinity involves the interplay of limitations at different cellular/tissue sites and different developmental phases. Depletion of SAMDC halves maximal photosynthesis under high salt (Mellidou et al., 2016). The AS-*ZmPAO* and S-*ZmPAO* with higher/lower PA titers, respectively, show no significant difference in the values of QY and CCI compared to WT at 0 DAT/0 mM NaCl, whereas transiently at 7 DAT/0 mM, both transgenics show greater A_{net} which nevertheless decreases at 14 DAT/0 mM NaCL (Fig. 3C). Under salt stress the more striking difference is the recovery from the osmotic/ionic stress the AS-*ZmPAO* plants show, which results to greater A_{net} at 50-200 mM NaCl/14 DAT. Overall, the results do not support in a consistent manner that the apoplastic PAO affects photosynthetic efficiency, at least during the examined stages of plant development.

In addition, the maintenance of cellular Na^+/K^+ homeostasis is pivotal for plant survival in saline environments. The effects of PAs on ionic pumps are pleiotropic (Pottosin, 2015; Pottossin and Shabala, 2014); for instance they block the FV and SV types of vacuolar cation channels. Externally applied PAs inhibit in roots the voltage-independent non-selective cation current (VI-NSCC), which is almost equally permeable to K^+ and Na^+, as well as to divalent cations (Ca^{2+}). Export and oxidation of PAs in the apoplast by PAO results in the induction of a novel ion conductance and confers Ca^{2+} influx across the plasma membrane, whereas PAs and ion channels cross-talk through the PAO-generated ROS (Pottosin, 2015; Pottosin and Shabala, 2014 and references therein). Deregulation of *PAO* gene results to higher/lower intracellular PA load in the AS-*ZmPAO*/S-*ZmPAO*, respectively, compared to WT. Under salinity the induced expression and the higher activity of PAO alters PA levels, with the AS-*ZmPAO* showing the higher Spd/Spm titers (Moschou et al., 2008a, b). These plants tend to contain lower Na^+ albeit not significantly different, but greater K^+, Ca^{2+}, and Mg^{2+} content than S-*ZmPAO* and WT in most salt doses and time-points (Fig. 4A,B,C,D). Increased K^+ content in the

shoots of plants under salinity has been often considered as a tolerance trait (Adem et al., 2014; Hariadi et al., 2011). Polyploid natural accessions in *Arabidopsis* show higher K^+ content in leaves, characteristic that correlates with NaCl tolerance, and attribute to the importance of high cytolosolic K^+ to suppress activity of caspase-like proteolytic and endonucleolytic enzymes triggering PCD. High cytosolic K^+ is also required to maintain metabolic processes, such as protein synthesis by enabling tRNA binding to ribosomes (Chao et al., 2013 and references therein). A strong negative correlation between the magnitude of salt-induced K^+ loss and salt tolerance, suggests K^+ retention as a selection criterion between salt tolerant and sensitive varieties (Chen et al., 2005, 2007a, 2007b; Lu et al., 2013; Smethurst et al., 2008). Increase of Ca^{2+} during abiotic and biotic stresses is required for tolerance in *Arabidopsis* (Johnson et al., 2014).

PA homeostasis is associated with activities of antioxidant enzymes (Mellidou et al., 2016). The mRNA levels of *CuZnSOD* are significantly higher in S-*ZmPAO* under salt conditions (Fig. 5A). *CAT1* mRNA level increases in S-*ZmPAO*, but does not decrease significantly in AS-*ZmPAO* (Fig. 5F). On the contrary, the cytoplasmic *APXc* mRNA levels show a positive correlation with the ROS levels post-treatment with NaCl, and seems to be leading antioxidant enzyme in the AS-*ZmPAO* plants (Fig. 5E) (Gémes et al., 2016; Moschou et al., 2008a, 2008b). The results suggest that PAO generates H_2O_2 that signals the expression of key enzymes in ROS scavenging/homeostasis, during the initial stages of salinity. Considering that SOD is a H_2O_2 producing enzyme, the increased SOD levels in AS-*ZmPAO* may reflect a homeostatic adjustment towards sustainment of H_2O_2 levels, while the increase of SOD in S-*ZmPAO* could reflect the increased $O_2^{\cdot -}$ content (Fig. 5A-D; Gémes et al., 2016; Moschou et al., 2008a, 2008b). Furthermore, total phenolics seem to be developmentally regulated with S-*ZmPAO* containing significantly higher total phenolics content (Fig. 6), consistent with the higher ROS load (Gémes et al., 2016; Moschou et al., 2008a, 2008b). However, there is no further accumulation of phenolics post-salt treatment consistent with the recent results that salt tolerance of the halophyte *Limonium delicatulum* is more associated with antioxidant enzyme activities than phenolic compounds (Souid et al., 2016).

Another interesting issue is the potential antagonistic relation between PAs and ethylene, with contrasting physiological effects/role(s) and the mutual regulatory link as they share a common precursor, S-adenosyl-L-methionine. PAs are considered as juvenility-related hormone-like substances (Paschalidis and Roubelakis-Angelakis, 2005a, 2005b, *inter alia*), whereas ethylene is a well-established senescence-inducing hormone.

Inhibition of ACC synthase decreases PAO-mediated H_2O_2 production during osmotic stress (Li et al., 2004), and PAO is strongly induced by ethylene (Gil-Amado and Gomez-Jimenez, 2012). PAO deregulation alters significantly the expression of the genes encoding ACC-synthase and ACC-oxidase. The AS-*ZmPAO* plants with the highest endogenous PA content (Moschou et al., 2008b) exhibit the highest mRNA levels of both genes under control and salinity conditions (Fig. 7). These results do not confirm that Spm regulates ethylene biosynthesis by inhibiting ACC-synthase (Li et al., 1992), whereas they fully support an antagonistic relationship between ethylene and PA pathways at the transcriptional level (Gil-Amado and Gomez-Jimenez, 2012). The AS-*ZmPAO* genotype with the highest titer of soluble Spm exhibits the highest level of *ACC-synthase* mRNA (Fig. 7) which links deregulation of PAO to ethylene synthesis.

Acclimation responses to salinity are often accompanied by the accumulation of proline, a common compatible osmolyte in plants. The accumulation of this amino acid is an important regulatory mechanism under osmotic stress (Huang et al., 2012). All tested genotypes accumulate proline under salinity and AS-*ZmPAO* seem to accumulate less proline (14 and 21 DAT, 200 mM NaCl) than the S-*ZmPAO* and WT (Fig. 8). When the biosynthetic pathway of PAs is altered, changes in cellular contents of PAs and proline often seem to occur in a coordinated manner rather than the two moving in opposite directions, even though their biosynthesis shares a common precursor, for example glutamate (Primikirios and Roubelakis-Angelakis, 1999; Mohapatra et al., 2010). Our results reinforce that PAO-generated ROS signal downstream expression of proline biosynthetic genes (Skopelitis et al., 2006). However, it is not clear whether or not increased proline biosynthesis is synthesized directly from glutamate by Δ^1-pyrroline-5-carboxylate synthetase (P5CS) or from ornithine by Ornithine aminotransferase. Overall, our data suggest that the level of expression of *PAO* exerts multifaceted effects under long-term salinity by affecting plant vigor *via* the modulation, to varying extent, of ion homeostasis, antioxidant machinery, phenolics, proline content and ethylene biosynthesis.

Cited Literature

Adem, G.D., Roy, S.J., Zhou, M., Bowman, J.P., Shabala, S., 2014. Evaluating contribution of ionic, osmotic and oxidative stress components towards salinity tolerance in barley. BMC Plant Biology 14,113. doi: 10.1186/1471-2229-14-113.

Andronis, E.A., Moschou, P.N., Toumi, I., and Roubelakis-Angelakis, K.A., 2014. Peroxisomal polyamine oxidase and NADPH-oxidase cross-talk for ROS homeostasis which affects respiration rate in *Arabidopsis thaliana*. Front. Plant Sci. 5, 132.

Bates, L., Waldren, R.P., Teare, I.D., 1973. Rapid determination of free proline for water-stress studies. Plant and Soil 39, 205-207.

Benzie, I.F., Chung, W.Y., and Strain, J.J., 1999. "Antioxidant" (reducing) efficiency of ascorbate in plasma is not affected by concentration. J. Nutr. Biochem.10, 146-150. doi: 10.1016/S0955-2863(98)00084-9.

Chao, D.Y., Dilkes, B., Luo, H.B., Douglas, A., Yakubova, E., Lahner, B., and Salt, D.E., 2013. Polyploids exhibit higher potassium uptake and salinity tolerance in Arabidopsis. Science 341, 658-659.

Chen, Z., Newman, I., Zhou, M., Mendham, N., Zhang, G., Shabala, S., 2005. Screening plants for salt tolerance by measuring K^+ flux: a case study for barley. Plant, Cell and Environm. 28, 1230-1246.

Chen, Z.H., Pottosin, II., Cuin, T.A., 2007a. Root plasma membrane transporters controlling K^+/Na^+homeostasis in salt-stressed barley. Plant Physiol. 145, 1714-1725.

Chen, Z.H., Zhou, M.X., Newman, I.A., Mendham, N.J., Zhang, G.P., Shabala, S., 2007b. Potassium and sodium relations in salinized barley tissues as a basis of differential salt tolerance. Funct. Plant Biol. 34, 150-162.

Davletova, S., Rizhsky, L., Liang, H., Shengqiang, Z., Oliver, D.J., Couty, J., Shulaev, V., Schlauch, K., Mittler, R., 2005. Cytosolic Ascorbate peroxidase1 is a central component of the reactive oxygen gene network in Arabidopsis. Plant Cell 17, 268-271.

Fujimoto, R., Taylor, J.M., Shirasawa, S., Peacock, W.J., and Dennis, E.S., 2012. Heterosis of Arabidopsis hybrids between C24 and Col is associated with increased photosynthesis capacity. Proc. Nat. L. Acad. Sci. USA 109, 7109-7114.

Gémes, K., Kim, Y.-J., Park, K.-Y., Moschou, P.N., Andronis, E., Valassaki, C., Roussis, A., Roubelakis-Angelakis, K.A., 2016. An NADPH-oxidase/Polyamine Oxidase feedback loop controls oxidative burst under salinity in *Nicotiana tabacum.* Plant Physiol., doi: 10.1104/pp.16.01118.

Gil-Amado, J.A., Gomez-Jimenez, M.C., 2012. Regulation of polyamine metabolism and biosynthetic gene expression during olive mature-fruit abscission. Planta 235, 1221-1237.

Hariadi, Y., Marandon, K., Tian, Y., Jacobsen, S.E., and Shabala, S., 2011. Ionic and osmotic relations in quinoa (*Chenopodium quinoa* Willd.) plants grown at various salinity levels. J. Exp. Bot. 62, 185-193.

Hou, Z.H., Liu, G.H., Hou, L.X., Wang, L.X., Liu, X., 2013. Regulatory function of polyaminoxidase-generated hydrogen peroxide in ethylene-induced stomatal closure in *Arabidopsis thaliana*. J. Integr. Agric. 12, 251-262.

Huang, W.L., Lee, C.H., Chen, Y.R., 2012. Levels of endogenous abscisic acid and indole-3-acetic acid influence shoot organogenesis in callus cultures of rice subjected to osmotic stress. Plant Cell Tiss. Organ Cult. 108, 257-263.

Johnson, J.M., Reichelt, M., Vadassery, J., Gershenzon, J., and Oelmuller, R., 2014. An Arabidopsis mutant impaired in intracellular calcium elevation is sensitive to biotic and abiotic stress. BMC Plant Biol. 14.

Kadoglidou, K., Chalkos, D., Karamanoli, K., Eleftherohorinos, I.G., Constantinidou, H.-I.A., and Vokou, D., 2014. Aromatic plants as soil amendments: Effects of spearmint and sage on soil properties, growth and physiology of tomato seedlings. Sci. Hortic. 179, 25-35.

Li, N., Parsons, B.L., Liu, D., Mattoo, A.K., 1992. Accumulation of wound-inducible ACC synthase transcript in tomato fruit is inhibited by salicylic acid and polyamines. Plant Mol. Biol. 18, 477-487.

Li, C.Z., Jiao, J., and Wang, G.X., 2004. The important roles of reactive oxygen species in the relationship between ethylene and polyamines in leaves of spring wheat seedlings under root osmotic stress. Plant Sci. 166, 303-315.

Lu, Y., Das, S.K., Moganty, S.S., and Archer, L.A., 2013. Ionic liquid-nanoparticle hybrid electrolytes and their application in secondary lithium-metal batteries. Adv. Mater. 24, 4430-4435.

Mattoo, A.K., Sobolev, A.P., Neelam, A., Goyal, R.K., Handa, A.K., Segre, A.L., 2006. Nuclear magnetic resonance spectroscopy based metabolite profiles of transgenic tomato fruit engineered to accumulate polyamines spermidine and spermine reveal enhanced anabolic nitrogen-carbon interactions. Plant Physiol. 142, 1759-1770.

McKay, H.M., 1998. Root electrolyte leakage and root growth potential as indicators of spruce and larch establishment. Silva Fennica 32(3), 241-252.

Mellidou, I., Moschou P.N., Pankou, Ch., Valassakis, Ch., Ioannidis, N., Gémes, K., Andronis, E.A., Roussis, A., Beris, D., Haralampidis, K., Karamanoli, A., Matsi, Th., Kotzabasis, K., Constantinidou, H-I., Roubelakis-Angelakis, K.A., 2016. *Nicotiana tabacum* plants with silenced S-Adenosyl-L-Methionine Decarboxylase (*SAMDC*) reveal a PA-dependent trade-off between growth and tolerance responses. Front. Plant Sci. doi: 10.3389/fpls.2016.00379.

Mohapatra, S., Minocha, R., Long, S., Minocha, R.C., 2010 Genetic manipulation of a single polyamine in poplar cells affects the accumulation of all amino acids. Amino Acids 38, 1117-1129.

Moschou, P.N., Roubelakis-Angelakis, K.A., 2014. Polyamines and programmed cell death. J. Exp. Bot. 65, 1285-1296.

Moschou, P.N., Delis, I.D., Paschalidis, K.A., and Roubelakis-Angelakis, K.A., 2008a. Transgenic tobacco plants overexpressing polyamine oxidase are not able to cope with oxidative burst generated by abiotic factors. Physiol. Plant. 133, 140-156.

Moschou, P.N., Paschalidis, K.A., Delis, I.D., Andriopoulou, A.H., Lagiotis, G.D., Yakoumakis, D.I., and Roubelakis-Angelakis, K.A., 2008b. Spermidine exodus and oxidation in the apoplast induced by abiotic stress is responsible for H_2O_2 signatures that direct tolerance responses in tobacco. Plant Cell 20, 1708-1724.

Moschou, P.N., Paschalidis, K.A., and Roubelakis-Angelakis, K.A., 2008c. Plant polyamine catabolism: The state of the art. Plant Signal. Behav. 3, 1061-1066.

Moschou, P.N., Sarris, P.F., Skandalis, N., Andriopoulou, A.H., Paschalidis, K.A., Panopoulos, N.J., Roubelakis-Angelakis, K.A., 2009. Engineered polyamine catabolism preinduces tolerance of tobacco to bacteria and oomycetes. Plant Physiology 149, 1970–1981.

Papadakis, A.K., and Roubelakis-Angelakis, K.A., 2005. Polyamines inhibit NADPH oxidase-mediated superoxide generation and putrescine prevents programmed cell death induced by polyamine oxidase-generated hydrogen peroxide. Planta 220, 826-837.

Paschalidis, K.A., Roubelakis-Angelakis, K.A., 2005a. Sites and regulation of polyamine catabolism in the tobacco plant. Correlations with cell division/expansion, cell cycle progression, and vascular development. Plant Physiol. 138, 2174-2184.

Paschalidis, K.A., Roubelakis-Angelakis, K.A., 2005b. Spatial and tem- poral distribution of polyamine levels and polyamine anabolism in different organs/tissues of the tobacco plant. Correlations with age, cell division/expansion, and differentiation. Plant Physiol. 138, 142-152.

Pottosin, I., 2015. Polyamine action on plant ion channels and pumps. *In*: Polyamines:A Universal Nexus for Growth, Survival, and Specialized Metabolism. T. Kusano and H. Suzuki (Eds), p. 229-241, Springer, ISBN 978-4-431-55211-6.

Pottosin, I., Shabala, S., 2014. Polyamines control of cation transport across plant membranes: implications for ion homeostasis and abiotic stress signaling. Front. Plant Sci. 5, 154.

Primikirios, N.I., Roubelakis-Angelakis, K.A., 1999. Cloning and expression of an arginine decarboxylase cDNA from *Vitis vinifera* L. cell-suspension cultures. Planta 208: 574-582.

Rodriguez, A.A., Maiale, M.J, Menendez, A.B., Ruiz, O.A., 2009. Polyamine oxidase activity contributes to sustain maize leaf elongation under saline stress. J. Exp. Bot. 60(15), 4249-62. doi: 10.1093/jxb/erp256.

Schneider, C.A., Rasband, W.S., and Eliceiri, K.W., 2012. NIH Image to ImageJ: 25 years of image analysis. Nat. Methods 9, 671-675.

Shabala, S., and Pottosin, I., 2014. Regulation of potassium transport in plants under hostile conditions: implications for abiotic and biotic stress tolerance. Physiol. Plant. 151, 257-279.

Shoresh, M., Spivak, M., Bernstein, N., 2011. Involvement of calcium-mediated effects on ROS metabolism in the regulation of growth improvement under salinity. Free Radic. Biol. Med. 51, 1221-1234. doi:10.1016/j.

Skopelitis, D.S., Paranychianakis, N.V., Paschalidis, K.A., Pliakonis, E.D., Delis, I.D., Yakoumakis, D.I., Kouvarakis, A., Papadakis, A.K., Stephanou, E.G., and Roubelakis-Angelakis, K.A., 2006. Abiotic stress generates ROS that signal expression of anionic glutamate dehydrogenases to form glutamate for proline synthesis in tobacco and grapevine. Plant Cell 18, 2767-2781.

Smethurst, C.F., Rix, K., Garnett, T., Auricht, G., Bayart, A., Lane, P., Wilson, S.J.., Shabala, S., 2008. Multiple traits associated with salt tolerance in lucerne: revealing the underlying cellular mechanisms. Funct. Plant Biol. 37, 640-650.

Souid, A., Gabriele, M., Longo, V.,Pucci, L., Bellani, L., Smaoui, A.,Abdelly, C., Ben Hamed, K. 2016. Salt tolerance of the halophyte *Limonium delicatulum* is more associated with antioxidant enzyme activities than phenolic compounds. Funct. Plant Biol.43(7), 607-619.

Swanson, S. and Gilroy, S., 2010. ROS in plant development. Physiol. Plant. 138, 384-392. doi:10.1111/j.1399-3054.2009.01313.x.

Tsiri, D., Chinou, I., Halabalaki, M., Haralampidis, K., and Ganis-Spyropoulos, C.G., 2009. The origin of copper-induced medicarpin accumulation and its secretion from roots of young fenugreek seedlings are regulated by copper concentration. Plant Sci. 176, 367-374. doi: 10.1016/j.plantsci.2008.12.001.

Urano, K., Hobo, T., Shinozaki, K., 2005. Arabidopsis ADC genes involved in polyamine biosynthesis are essential for seed development. FEBS Lett. 579, 1557-1564.

Wi, S.J. and Park, K.Y., 2002. Antisense expression of carnation cDNA encoding ACC synthase or ACC oxidase enhances polyamine content and abiotic stress tolerance in transgenic tobacco plants. Mol Cells 13, 209–220.

Yamaguchi, K., Takahashi, Y., Berberich, T., Imai, A., Miyazaki, A., Takahashi, T., Michael, A., Kusano, T., 2006. The polyamine spermine protects against high salt stress in *Arabidopsis thaliana*. FEBS Lett. 580, 6783–6788.

Yoda, H., Hiroi, Y., Sano, H., 2006. Polyamine oxidase is one of the key elements for oxidative burst to induce programmed cell death in tobacco cultured cells. Plant Physiol. 142, 193-206.

LEGENDS OF FIGURES

Figure 1. Phenotypic characteristics of WT, AS-*ZmPAO* and S-*ZmPAO* transgenic plants under 0, 50, 100, 200, 300 mM at 0, 7, 14 and 21 DAT. **(A)** Plant height; **(B)** Number of leaves; **(C)** Leaf area. Data are means±SE of three biological replicates with three technical replicates each. Different letters indicate significant differences of Duncan's multiple comparisons ($P<0.05$).

Figure 2. Plant biomass of WT, AS-*ZmPAO* and S-*ZmPAO* transgenic plants under 0, 50, 100, 200, 300 mM at 0, 7, 14 and 21 DAT. **(A)** Fresh weight; **(B)** Dry weight. Data are means±SE of three biological replicates with three technical replicates each. Different letters indicate significant differences of Duncan's multiple comparisons ($P<0.05$).

Figure 3. Photosynthetic parameters in the leaves of WT, AS-*ZmPAO* and S-*ZmPAO* transgenic plants under 0, 50, 100, 200, 300 mM at 0, 7 and 14 DAT. **(A)** Photosynthetic yield (QY), **(B)** Chlorophyll content index (CCI), and **(C)** Net photosynthetic rate (A_{net}). Data are means±SE of three biological replicates with three technical replicates each. Different letters indicate significant differences of Duncan's multiple comparisons ($P<0.05$).

Figure 4. Ion content (Na^+, K^+, Ca^{2+}, Mg^{2+}) in the leaves of WT, AS-*ZmPAO* and S-*ZmPAO* transgenic tobacco plants under 0, 200, 300 mM at 0, 14 and 21 DAT. (A) Na^+ content; **(B)** K^+ content; **(C)** Ca^{2+} content; **(D)** Mg^{2+} content. Data are means±SE of three biological replicates with three technical replicates each. Different letters indicate significant differences of Duncan's multiple comparisons ($P<0.05$).

Figure 5. Superoxide dismutases, Catalase and Ascorbate peroxidase in WT, AS-*ZmPAO* and S-*ZmPAO* transgenic plants under control and post-salt treatment.
(A) Abundance of mRNA levels of chloroplastic *CuZnSOD* in the leaves post-salt treatment with 200 mM NaCl. **(B-D)** In-gel activity of chloroplastic FeSOD (B lower band**, C)** and mitochondrial MnSOD (B upper band; D) isoenzymes in the leaves 24 h post-salt treatment with 200 mM NaCl. **(E)** Abundance of mRNA levels of *APX* encoding the cytosolic APX in the leaves post-salt treatment with 200 mM NaCl. **(F)** Abundance of mRNA levels of *CAT* in the leaves post-salt treatment with 200 mM NaCl. Data are means±SE of three biological replicates with three technical replicates each. Different letters indicate significant differences of Duncan's multiple comparisons ($P<0.05$).

Figure 6. Total phenolics in the leaves of WT, AS-*ZmPAO* and S-*ZmPAO* transgenic plants. (A) Total phenolics in the leaves 0, 7, 14 days post-salt treatment with 100 mM NaCl. **(B)** Total phenolics in the leaves 0, 7, 14 days post-salt treatment with 100 mM mannitol. **(C)** Qualitative analysis of total phenolics by TLC in the leaves 24 h post-salt treatment with 100 mM NaCl. Images are from a single representative experiment replicated three times. **(D)** Antioxidant capacity (Ascorbic acid Equivalents, AAE) in the leaves under control and 7 DAT with 100 mM NaCl. Data are means±SE of three

biological replicates with three technical replicates each. Different letters indicate significant differences of Duncan's multiple comparisons (P<0.05).

Figure 7. Ethylene biosynthetic genes in WT, AS-*ZmPAO* and S-*ZmPAO* plants under control and post-salt treatment with 200 mM NaCl. (A) Abundance of mRNA levels of *ACC synthase*. **(B)** Abundance of mRNA levels of *ACC oxidase*. Each experiment was repeated three times. Data are means±SE of three biological replicates with three technical replicates each. Different letters indicate significant differences of Duncan's multiple comparisons (P<0.05).

Figure 8. (A) Proline content (L-proline equivalents, PE) and (B) Root electrolyte leakage (%) in the roots of WT, S-*ZmPAO* and AS-*ZmPAO* transgenic plants under 0, 200 and 300 mM at 0, 7, 14 and 21 DAT. Data are means±SE of three biological replicates with three technical replicates each. Different letters indicate significant differences of Duncan's multiple comparisons (P<0.05).

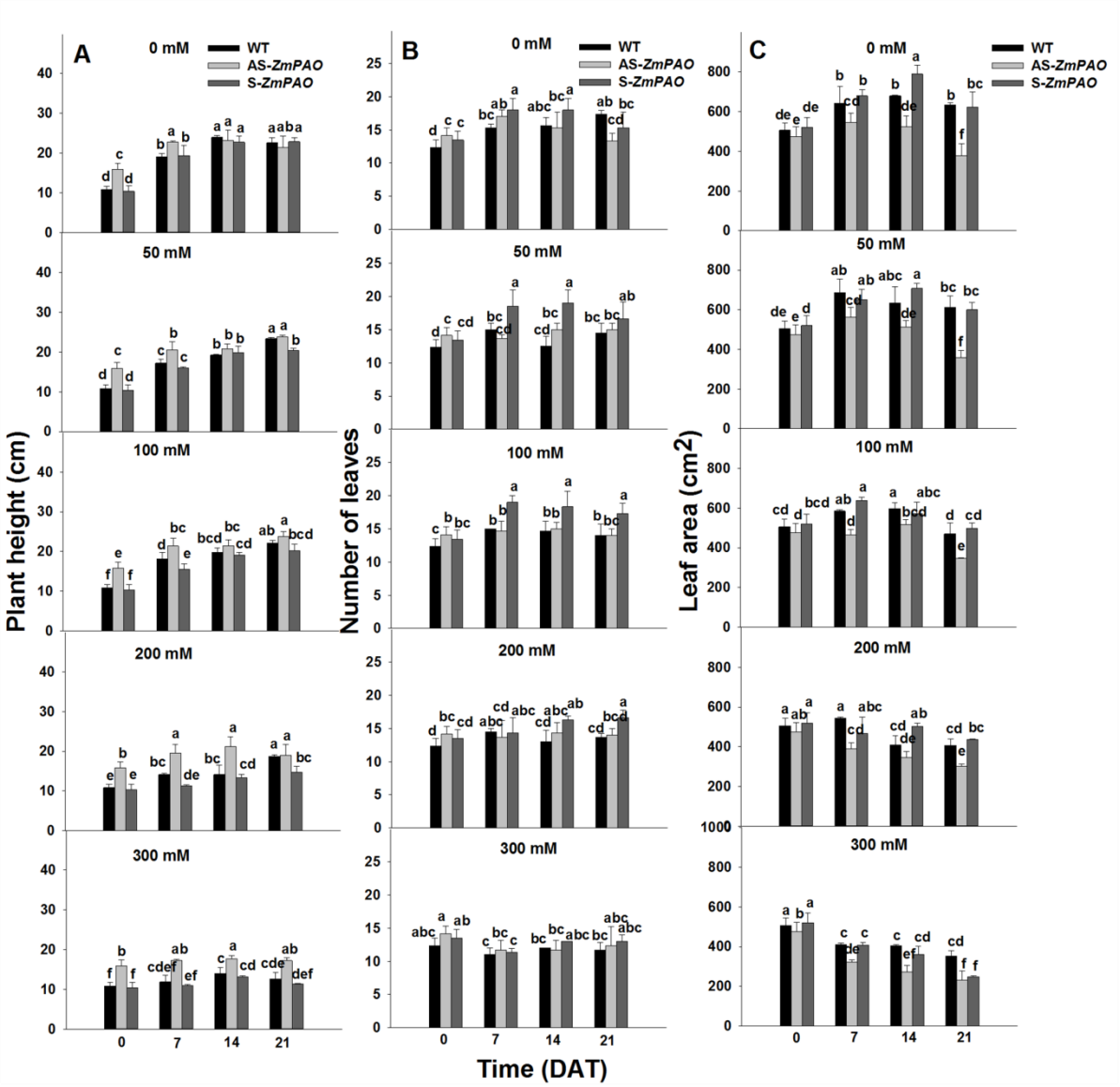

Figure 1. Phenotypic characteristics of WT, AS-*ZmPAO* and S-*ZmPAO* transgenic plants under 0, 50, 100, 200, 300 mM at 0, 7, 14 and 21 DAT. **(A)** Plant height; **(B)** Number of leaves; **(C)** Leaf area. Data are means±SE of three biological replicates with three technical replicates each. Different letters indicate significant differences of Duncan's multiple comparisons ($P<0.05$).

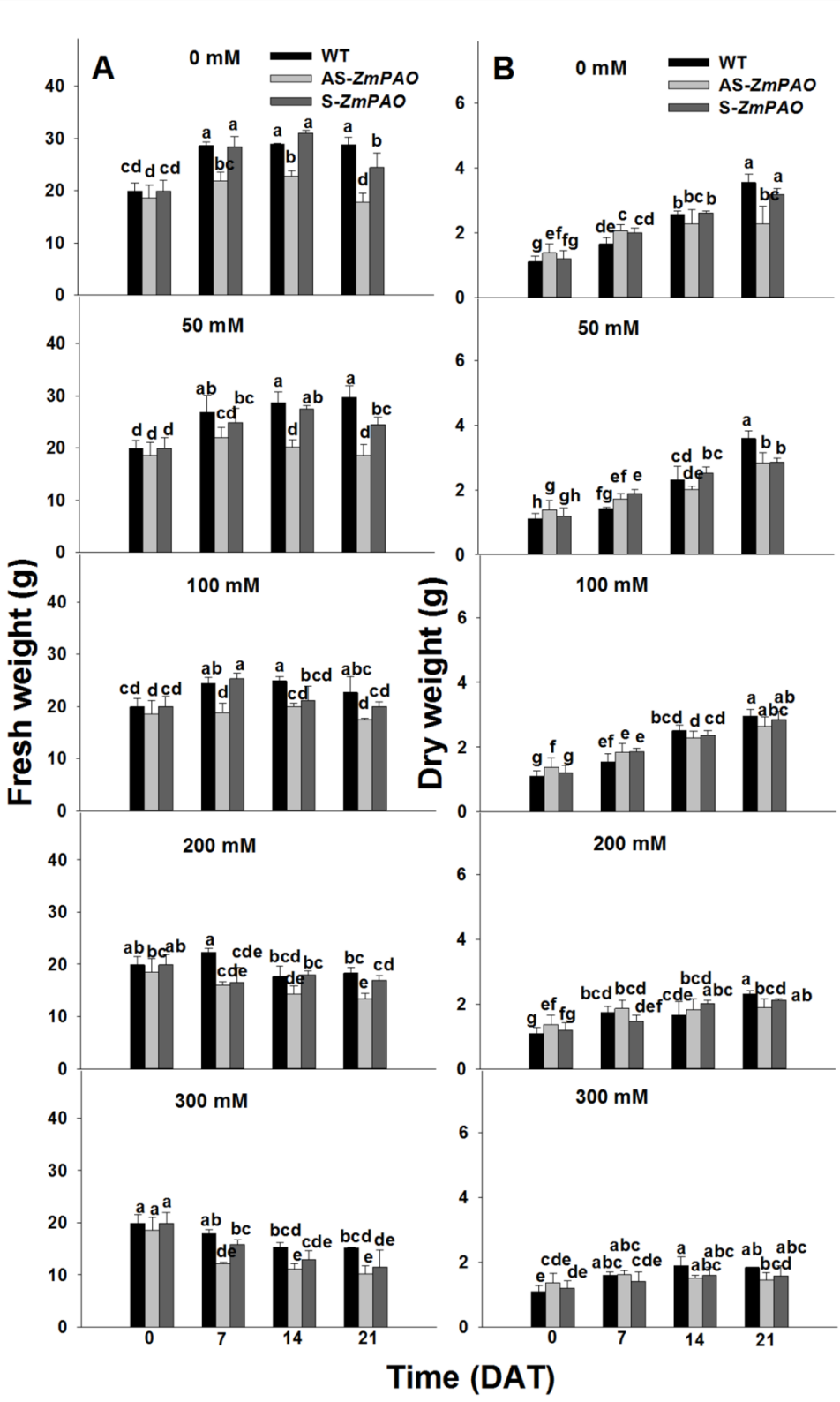

Figure 2. Plant biomass of WT, AS-*ZmPAO* and S-*ZmPAO* transgenic plants under 0, 50, 100, 200, 300 mM at 0, 7, 14 and 21 DAT. **(A)** Fresh weight; **(B)** Dry weight. Data are means±SE of three biological replicates with three technical replicates each. Different letters indicate significant differences of Duncan's multiple comparisons ($P<0.05$).

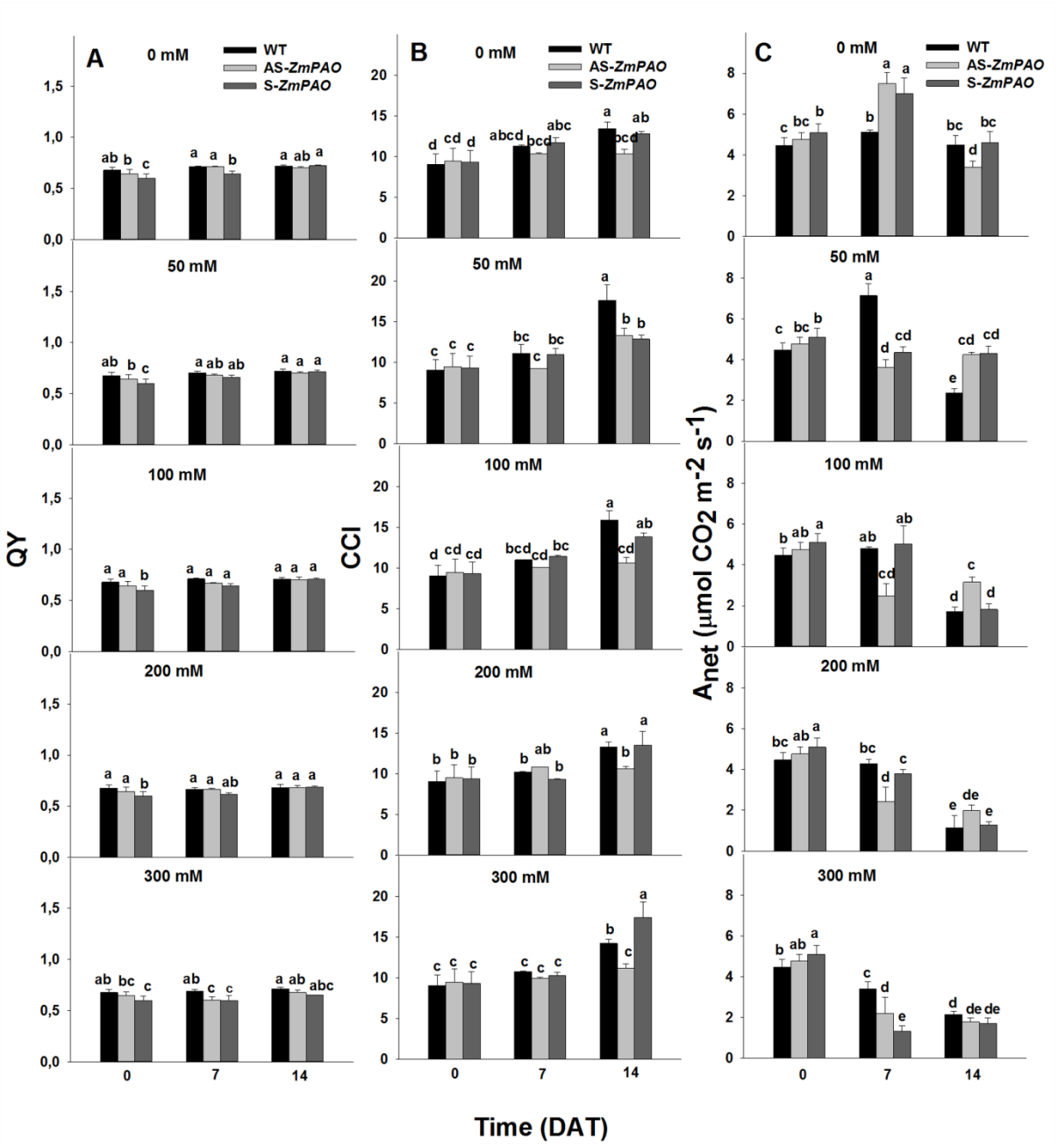

Figure 3. Photosynthetic parameters in the leaves of WT, AS-*ZmPAO* and S-*ZmPAO* transgenic plants under 0, 50, 100, 200, 300 mM at 0, 7 and 14 DAT. **(A)** Photosynthetic yield (QY); **(B)** Chlorophyll content index (CCI); and **(C)** Net photosynthetic rate (A_{net}). Data are means±SE of three biological replicates with three technical replicates each. Different letters indicate significant differences of Duncan's multiple comparisons ($P<0.05$).

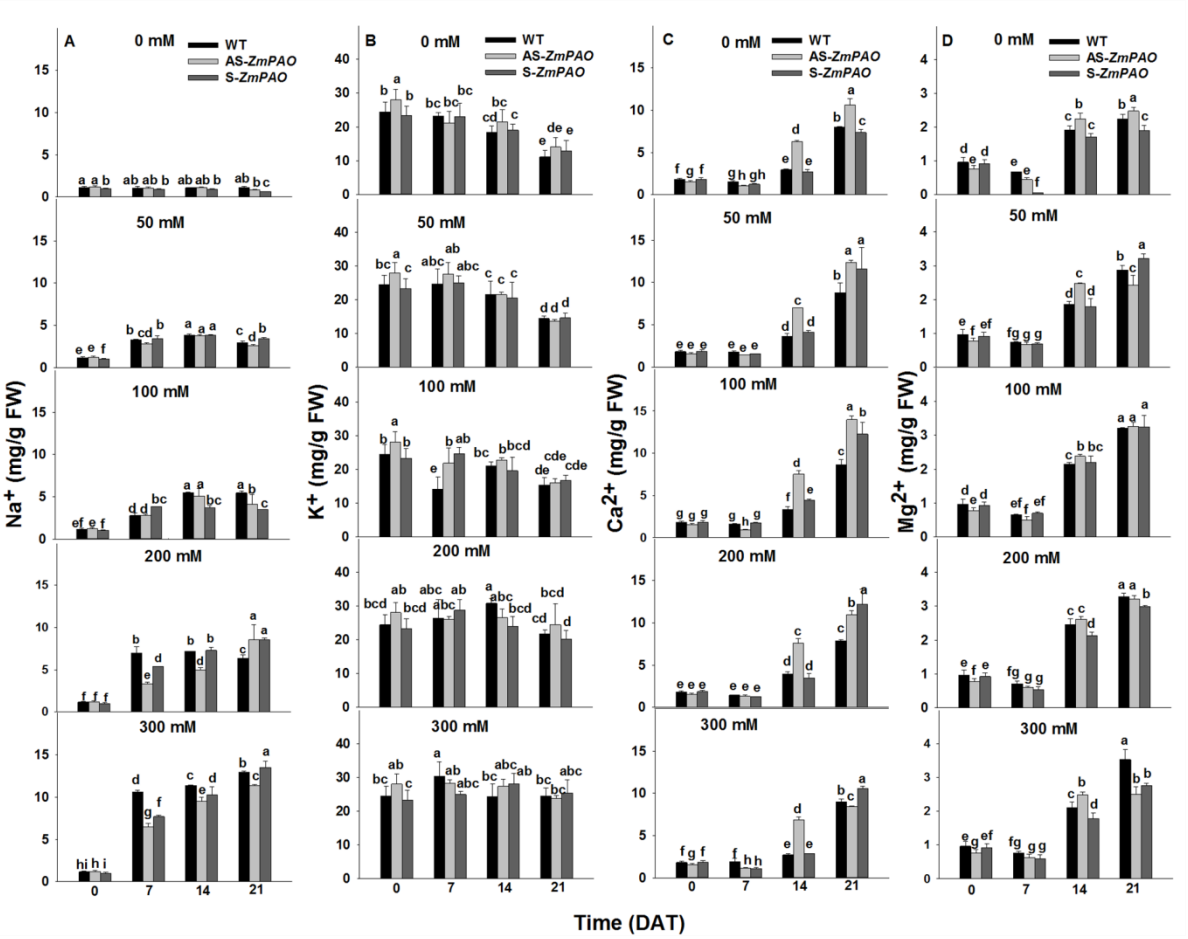

Figure 4. Ion content (Na^+, K^+, Ca^{2+}, Mg^{2+}) in the leaves of WT, AS-*ZmPAO* and S-*ZmPAO* transgenic tobacco plants under 0, 50, 100, 200 and 300 mM at 0, 7, 14 and 21 DAT. (A) Na^+ content; **(B)** K^+ content; **(C)** Ca^{2+} content; and **(D)** Mg^{2+} content. Data are means±SE of three biological replicates with three technical replicates each. Different letters indicate significant differences of Duncan's multiple comparisons ($P<0.05$).

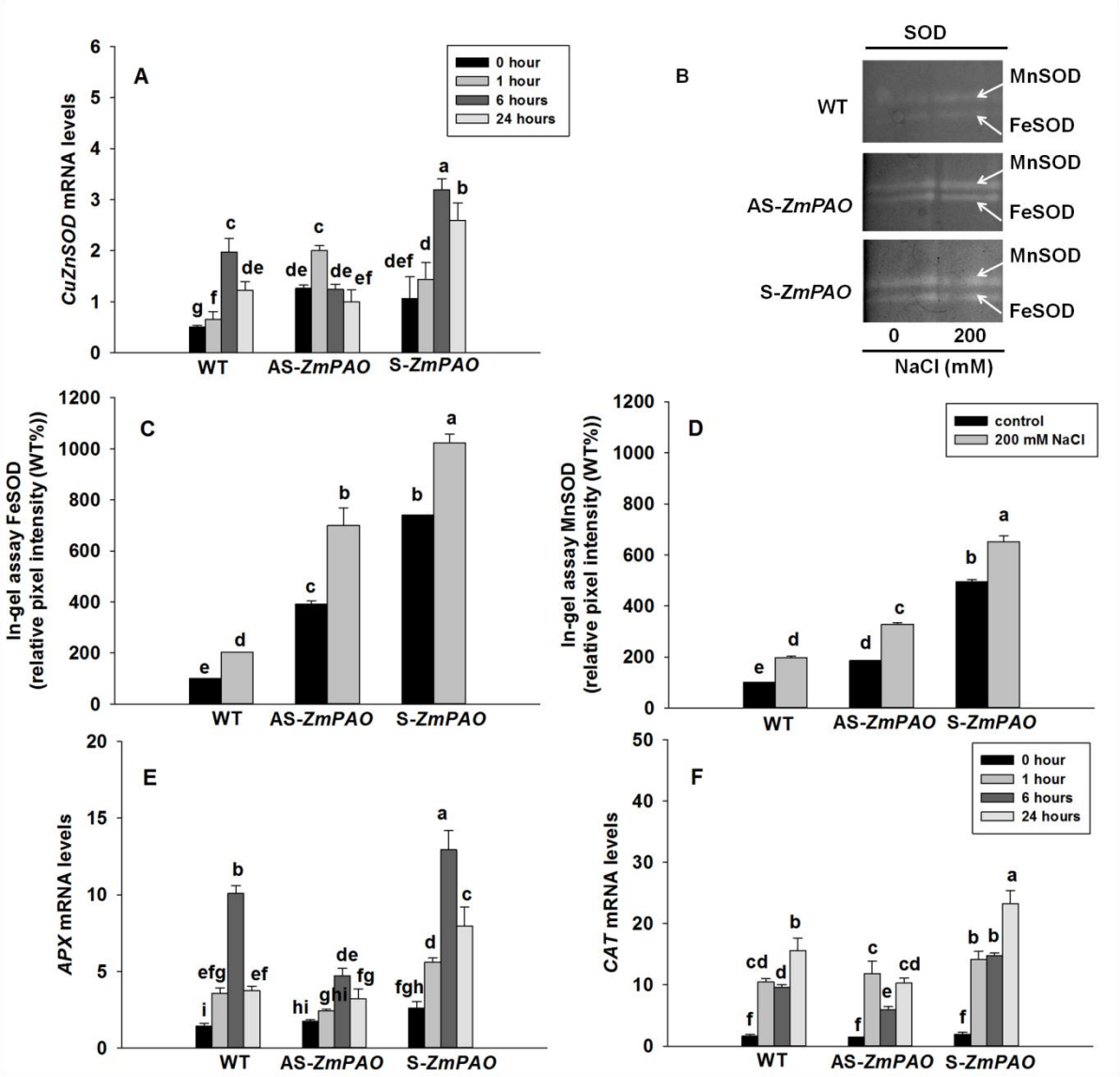

Figure 5. Superoxide dismutases, Catalase and Ascorbate peroxidase in WT, AS-*ZmPAO* and S-*ZmPAO* transgenic plants under control and post-salt treatment.

(A) Abundance of mRNA levels of chloroplastic *CuZnSOD* in the leaves post-salt treatment with 200 mM NaCl. **(B-D)** In-gel activity of chloroplastic FeSOD (B lower band; **C)** and mitochondrial MnSOD (B upper band; **(D)** isoenzymes in the leaves 24 h post-salt treatment with 200 mM NaCl; **(E)** Abundance of mRNA levels of *APX* encoding the cytosolic APX in the leaves post-salt treatment with 200 mM NaCl; **(F)** Abundance of mRNA levels of *CAT* in the leaves post-salt treatment with 200 mM NaCl. Data are means±SE of three biological replicates with three technical replicates each. Different letters indicate significant differences of Duncan's multiple comparisons ($P<0.05$).

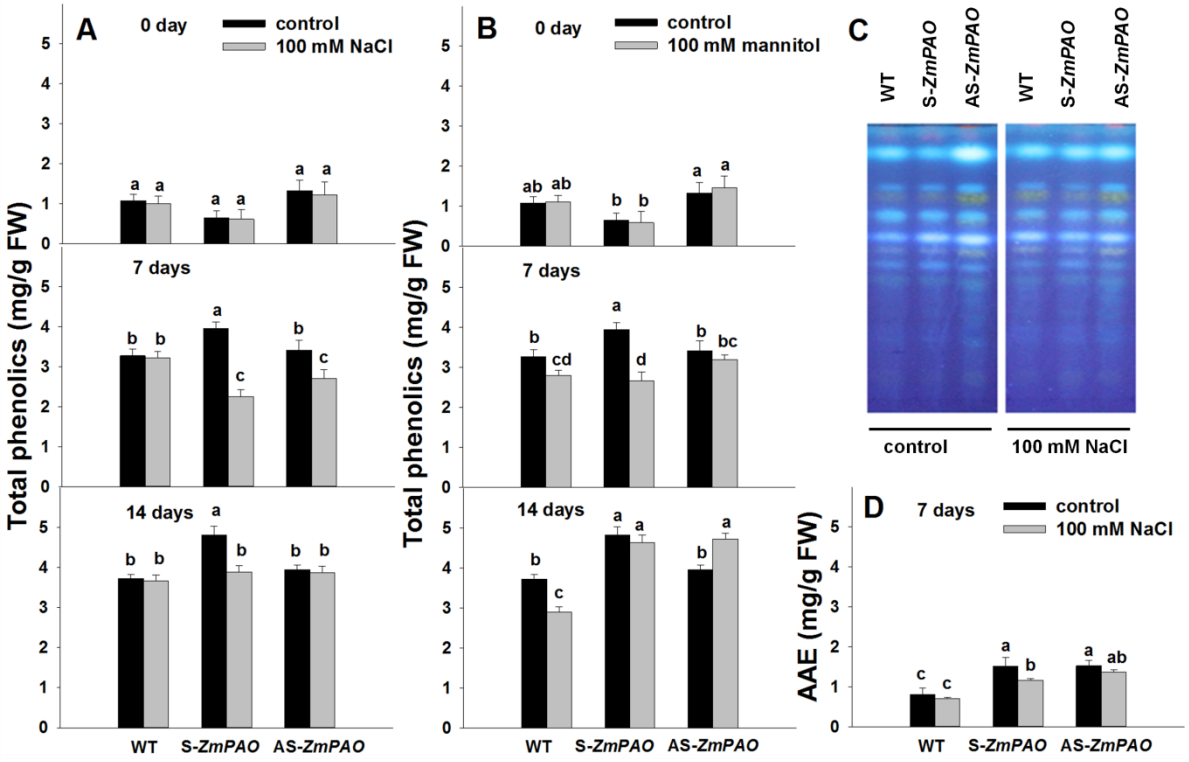

Figure 6. Total phenolics in the leaves of WT, AS-*ZmPAO* and S-*ZmPAO* transgenic plants. (A) Total phenolics in the leaves 0, 7, 14 days post-salt treatment with 100 mM NaCl; **(B)** Total phenolics in the leaves 0, 7, 14 days post-salt treatment with 100 mM mannitol; **(C)** Qualitative analysis of total phenolics by TLC in the leaves 24 h post-salt treatment with 100 mM NaCl. Images are from a single representative experiment replicated three times; **(D)** Antioxidant capacity (Ascorbic acid Equivalents, AAE) in the leaves under control and 7 DAT with 100 mM NaCl. Data are means±SE of three biological replicates with three technical replicates each. Different letters indicate significant differences of Duncan's multiple comparisons ($P<0.05$).

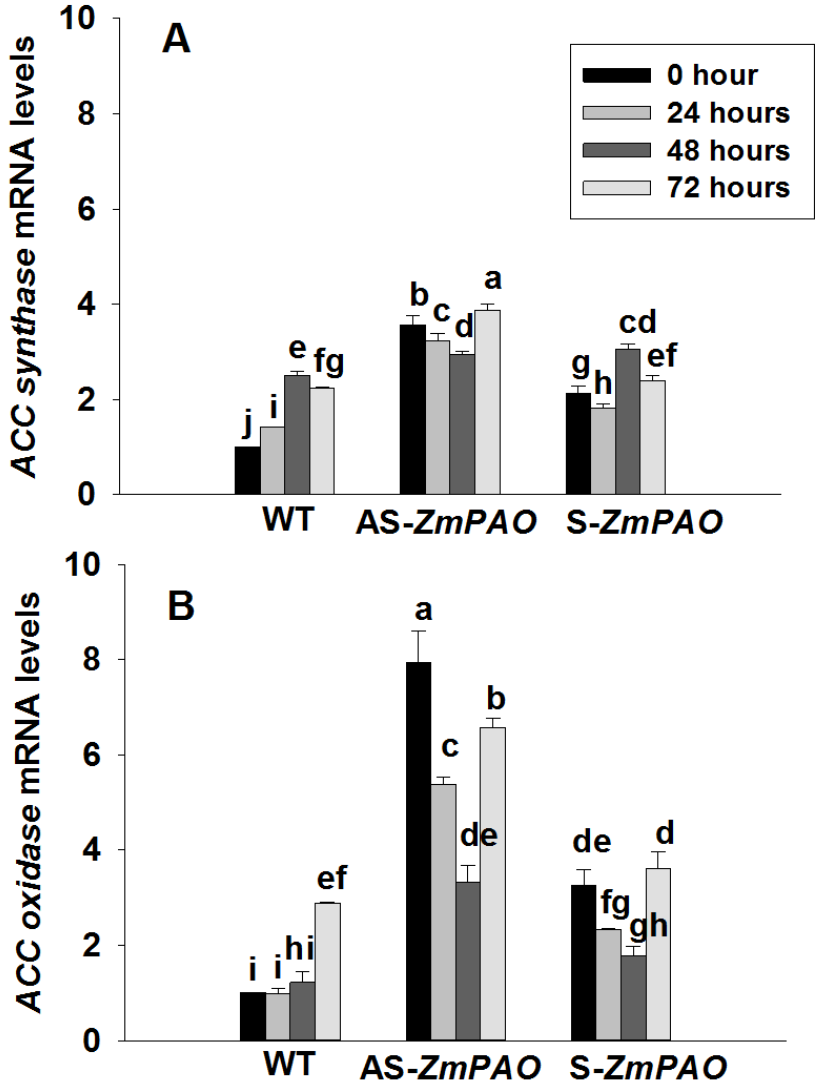

Figure 7. Ethylene biosynthetic genes in WT, AS-*ZmPAO* and S-*ZmPAO* plants under control and post-salt treatment with 200 mM NaCl. (A) Abundance of mRNA levels of *ACC-synthase*; **(B)** Abundance of mRNA levels of *ACC-oxidase*. Each experiment was repeated three times. Data are means±SE of three biological replicates with three technical replicates each. Different letters indicate significant differences of Duncan's multiple comparisons ($P<0.05$).

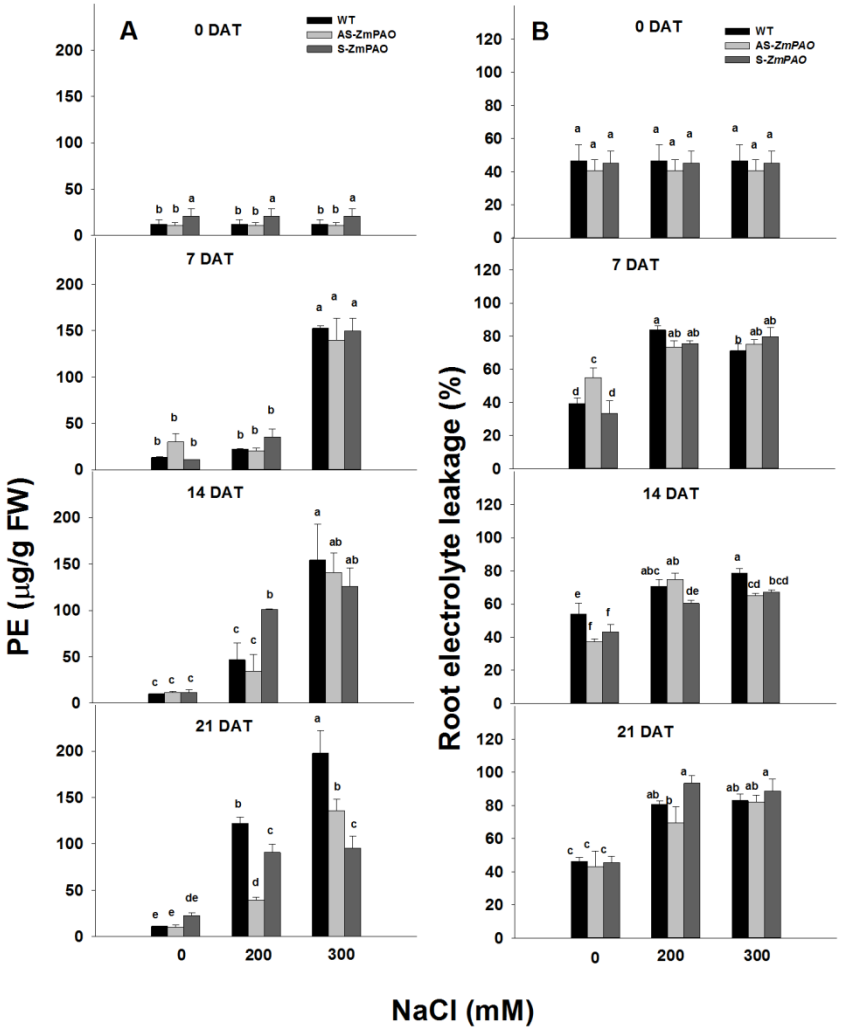

Figure 8. (A) Proline content (L-proline equivalents, PE) and (B) Root electrolyte leakage (%) in the roots of WT, S-*ZmPAO* and AS-*ZmPAO* transgenic plants under 0, 200 and 300 mM at 0, 7, 14 and 21 DAT. Data are means±SE of three biological replicates with three technical replicates each. Different letters indicate significant differences of Duncan's multiple comparisons ($P<0.05$).